

Complicated surface structure of flower-like bunches of $\text{LiV}_{0.1}\text{Mn}_{1.9}\text{O}_4$ nanofibers

ALI EFTEKHARI*, FATHOLLAH MOZTARZADEH and
MAHMOOD KAZEMZAD

Laboratory of Electrochemistry, Materials and Energy Research Center,
P.O. Box 14155-4777, Tehran, Iran

(Received October 2005; in final form December 2005)

$\text{LiV}_{0.1}\text{Mn}_{1.9}\text{O}_4$ nanofibers were synthesized via a conventional solid-state reaction. The nanofibers tend to form bunches with flower-like shapes. Since this interesting form provides a 3D structure, surface analysis of such flowers is of particular interest and was performed by means of small-angle X-ray scattering (SAXS) via the concept of fractal geometry. The results obtained from experimental measurements suggested a fractal dimension close to 3, which is indicative of a 3D structure. This provides an excellent accessibility of the material for diffusion-based reactions, since diffusion within the material is easy through such ordered nanofibers.

Keywords: Nanofibers; Nanostructured flowers; Fractal dimension; SAXS; LiMn_2O_4 ; Lithium battery

1. Introduction

Fabrication of nanostructured materials is an advancing and rapidly growing area of research due to their important applications. An example is one-dimensional nanomaterials such as nanofibers, nanotubes, nanowires, nanorods, etc. In addition to their preparation, an important task of nanotechnology is to bunch such one-dimensional nanomaterials to achieve a suitable form for applied purposes. For instance, template-based methods are common for the preparation of porous materials [1–3]. This provides a superior activity for materials involving diffusion-based reactions, since diffusion through ordered nanostructures is easy [4].

Lithium batteries are an important type of power sources with potential applications for various purposes. They play an important role in modern technology, particularly miniaturized technologies. LiMn_2O_4 is a promising candidate for future development of lithium batteries, due to its valuable advantages for commercialization (e.g., non-toxicity, low-cost, etc). As the most successful route for synthesis of LiMn_2O_4 is solid-state reaction, it is difficult to synthesize it in the form of one-dimensional

*Corresponding author. Email: eftekhari@merc.ac.ir

nanomaterials. On the other hand, placing synthesised sample into conventional alumina template to build nanowires is a difficult and time-consuming process [5, 6]. Here, we report a truly simple method for direct synthesis of LiMn_2O_4 nanofibers (which are significantly smaller than nanowires prepared by template-based methods). Since this is accompanied by the formation of a novel form of nanofibers bunches, we pay our attention to surface analysis of it, which reveal new opportunities for future researches.

2. Experimental

The solid-state synthesis was performed by 8 h heating at 500°C following by 40 h heating at 800°C of a mixture of stoichiometric amounts of MnO_2 , Li_2CO_3 , and V_2O_5 . The heating process at 500°C is very important, since V_2O_5 will be melted at higher temperatures. In fact, this is an obstacle for the synthesis of $\text{LiV}_x\text{M}_{2-x}\text{O}_4$ when x is high. The sample was slowly cooled to the room temperature. Scanning electron microscopy (SEM) investigations were carried out using a Cambridge electron microscope, model Steroscan 360.

Small-angle X-ray scattering (SAXS) investigations were carried out using a Philips PW-3710 diffractometer employing a rotating X-ray source under appropriate conditions. Interestingly, SAXS measurements can be simply employed to inspect nanostructures smaller than 20 nm. Whereas, the difficulties for performing SAXS experiments is related to larger scale where the scattering should be done at very small angles (which may be accompanied by severe errors depending on the apparatus sensitivity).

3. Results and discussion

Substitution of Mn by transition metals is a common approach to improve battery performance of LiMn_2O_4 cathodes [7–13]. Although various elements have been employed for this purpose, less attention has been paid to vanadium. This failure can be attributed to the fact that vanadium oxide has a low melting point, and V is a pentavalent cation which decreases the valance of Mn (i.e. unfavorable). According to the above-mentioned experimental procedure, small amount of V will be incorporated into the LiMn_2O_4 lattice before V_2O_5 melting. On the other hand, Chitrakar *et al.* have shown that even pentavalent cations do not necessarily decrease the Mn valence [12]. In other words, incorporating V into LiMn_2O_4 lattice is a favorable action, and it is a double advantage to use this approach to fabricate nanostructured material.

The XRD pattern of the $\text{LiV}_{0.1}\text{Mn}_{1.9}\text{O}_4$ sample (figure 1) clearly confirms successful synthesis process via the above-mentioned solid-state route. It is similar to the XRD pattern of conventional LiMn_2O_4 , suggesting a conventional spinel with the space group of $Fd3m$. No noticeable peak corresponding to impurities is observable. It is known that incorporation of small amount of transition metals into the LiMn_2O_4 lattice does not change the lattice structure (just a slight change in the lattice constant). The $\text{LiV}_{0.1}\text{Mn}_{1.9}\text{O}_4$ sample also shows a similar electrochemical activity in respect with the lithium ion insertion/extraction as well as LiMn_2O_4 [14]. However, this is the

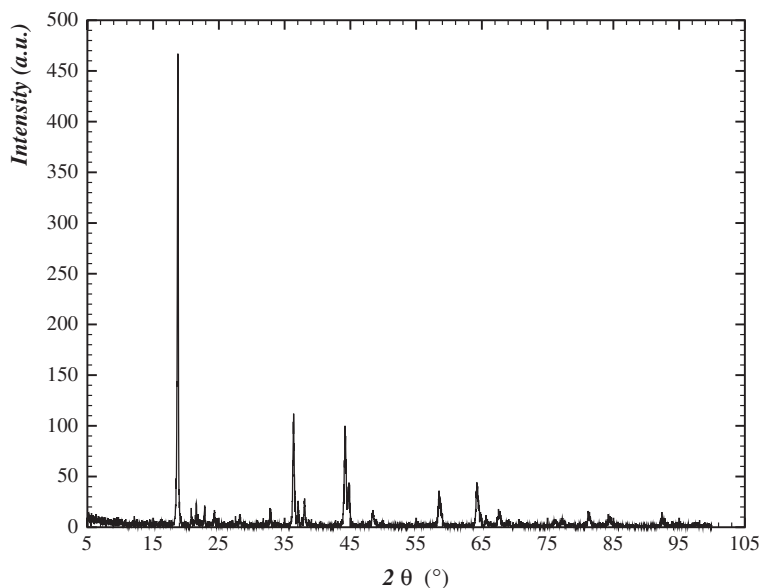


Figure 1. XRD pattern of the $\text{LiV}_{0.1}\text{Mn}_{1.9}\text{O}_4$ sample synthesized by the conventional solid-state reaction.

subject of another detailed study with a different aspect [15]. Here, we concentrate on the extraordinary morphology of the $\text{LiV}_{0.1}\text{Mn}_{1.9}\text{O}_4$ nanofibers synthesized. In fact, formation of unexpected morphologies is likely in synthesis of this class of materials [16, 17].

Various features of the nanostructures of $\text{LiV}_{0.1}\text{Mn}_{1.9}\text{O}_4$ sample as revealed by means of electron microscopy are illustrated in figure 2. It is obvious that insertion of (even small amount of) V into the LiMn_2O_4 lattice changes the morphology to form nanofibers instead of conventional microparticles (figure 2A). Formation of such nanofibers without any special procedure just via a simple solid-state synthesis is of particular interest from nanotechnology point of view. These nanofibers are in the range of 10–50 nm in diameter, though there is a strong tendency for adhering together to form larger nanofibers. Another interesting feature of this phenomenon is alignment of such nanofibers in one direction (figure 2B). Thus, huge bunches of nanofibers are formed. The total sizes of such bunches are from decades to hundreds of micrometers. This provides an opportunity for easy handling of them.

In spite of the unusual phenomena reported above, a truly extraordinary phenomenon was also observed for this case leading to the formation of a new form of nanostructured materials. In addition to alignment of individual nanofibers to form ordered bunches, they tend to form flower-like structures (figure 2C and D). It is still very soon to propose an exact mechanism for the occurrence of such extraordinary phenomenon. However, it is believed that this is due to significant suppleness and blending capacity of such narrow nanofibers. In solid-state synthesis, material morphology is usually originated from solid-state diffusion. However, this is not responsible for the system under investigation, since hydrothermal synthesis also leads to the formation of $\text{LiV}_{0.1}\text{Mn}_{1.9}\text{O}_4$ nanofibers [15].

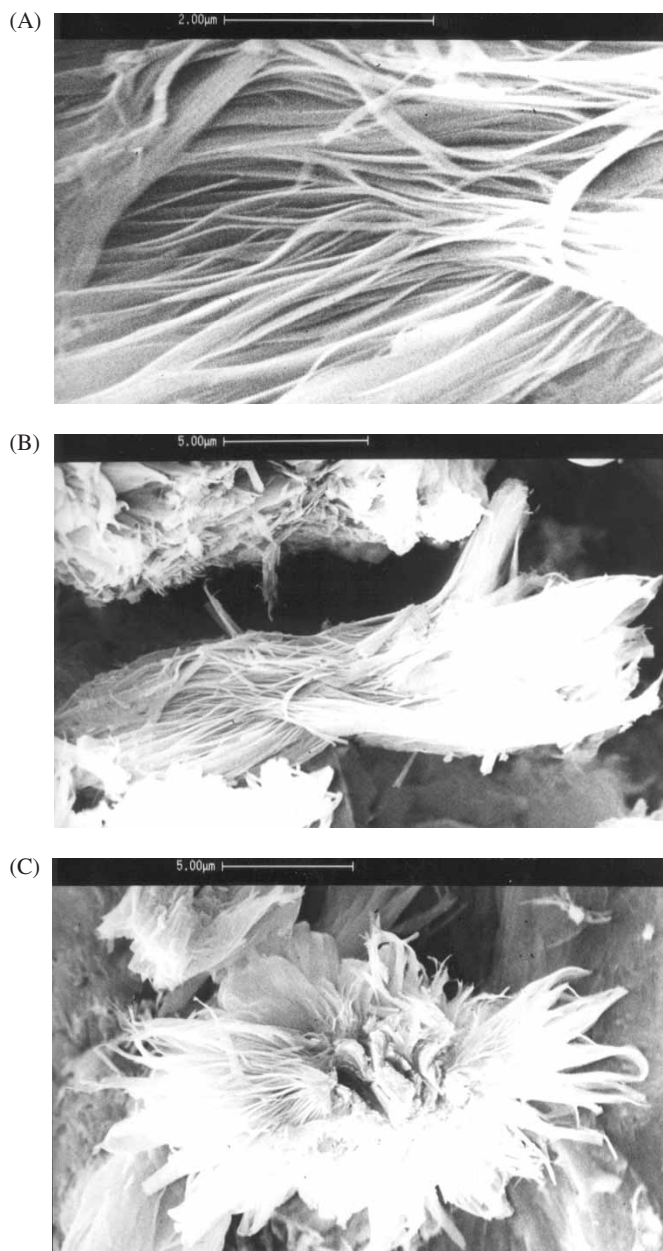


Figure 2. Typical SEM images of different places of the $\text{LiV}_{0.1}\text{Mn}_{1.9}\text{O}_4$ sample. They illustrate various flower-like bunches formed in the course of just a simple solid-state reaction.

According to the morphology of various parts of the sample (figure 2), it can be concluded that the aligned nanofibers may keep their straightness to form ordered bunches (figure 2A and B) or may be opened as an opening bud (figure 2C and D). In the latter case, a spherical shape is generated due to bended nanofibers.

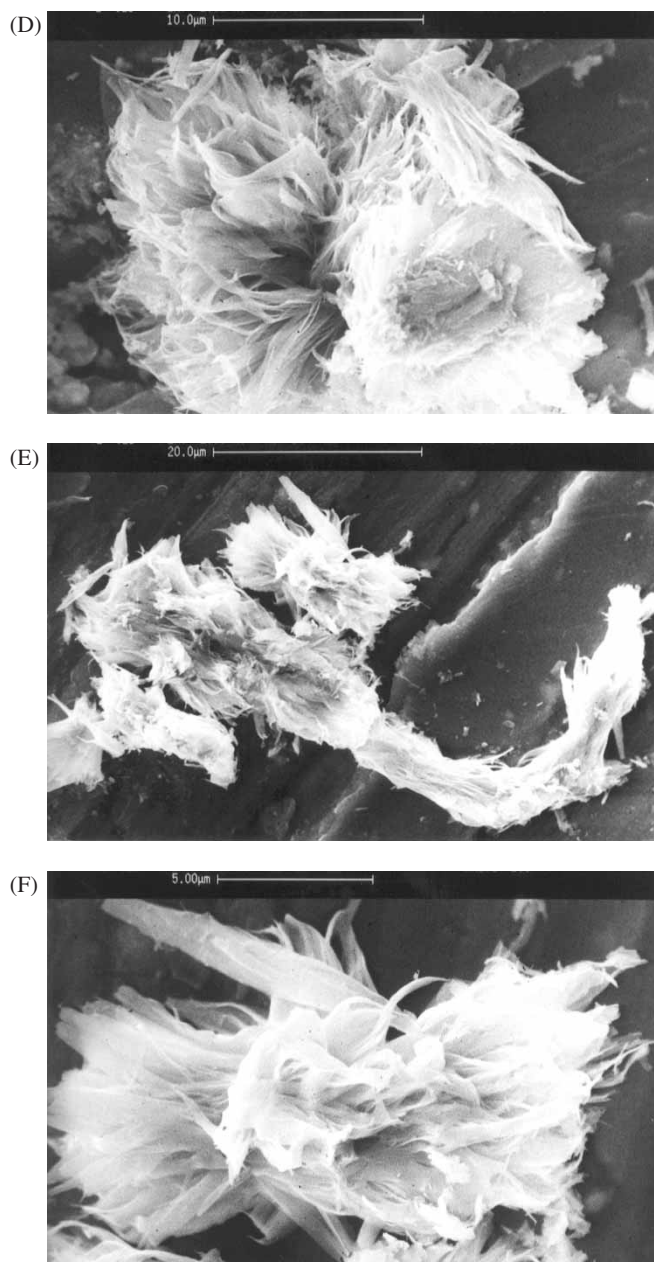


Figure 2. Continued.

The controlling factor for the occurrence of these two cases is the topological position of them in the solid-state medium. It is difficult to dominate this factor due to randomness of the solid-state medium employed for the synthesis process. This randomness may lead to the formation of various objects (c.f. figure 2E and F).

However, formation of such flower-like bunches of nanofibers is indeed an interesting phenomenon deserving a particular attention to investigate its complicated structure. It is the task of surface science to reveal surface structure of such spherical bunches of nanofibers, which have flower-like shapes.

Since this nanostructured material is not a flat surface, it is not possible to investigate its lateral structure by means of conventional scanning probe microscopy (SPM) techniques. Transmission-based techniques such as transmission electron microscopy (TEM) are also inappropriate due to huge size of flower-like bunches. We also encountered this problem in study of bunches of manganese oxide nanowires [16]. On the other hand, study of a similar system indicated that TEM images are not representative of nanostructures, and other reliable techniques are necessary to judge in this context [18]. Here, we wish to gain a powerful technique for a general study of the peculiar nanostructure obtained by vanadium insertion into LiMn_2O_4 spinel.

In the mean time, according to the typical SEM images (figure 2), different shapes are formed and a single local surface analysis is not representative of the phenomenon. Thus, we use an efficient technique to obtain a statistical data owing to all regions of the surfaces. Small-angle X-ray scattering (SAXS) is one of the most reliable techniques for surface analysis in the scale of 0.5–200 nm [19]. Of course, preparation of such samples for SAXS experiments is difficult, but these spherical bunches are sufficiently large for easy handling. On the other hand, in our experience, such flower-like bunches tends to stand vertically (as illustrated in figure 2D). However, SAXS measurements provide a statistical analysis of the whole sample.

It is well known that scattering intensity mainly includes [20]: the diffuse scattering, and the Porod term. The last term represents the surface roughness. The Porod term is accompanied by a sharp rise of the intensity in the small-angle region, which is indicative of density fluctuations on nanoscale. The Porod term correspond to the material structure on a scale from about 0.5 through 200 nm. In this region, the Porod power-law suggests: $I(q) \propto q^{-\beta}$, where β depends on the material form (e.g. mass or surface), and for fractal surfaces is equal to $6 - D$ [21]. However, this relation is only valid when the scattering intensity is mainly due to the Porod term. As Ruland [22] pointed out the validity of Porod's law should be taken into account for fractal analysis, and indeed an appropriate scale should be used for collecting the data.

It is a great opportunity to estimate the fractal dimension, since it provides a geometrical significance for the surface analysis. By this approach, it is possible to obtain a geometrical measure of the structure's complexity [23, 24]. To this aim, the SAXS intensities were plotted against the q factor in a logarithmic scale (figure 3). This typical SAXS analysis corresponds to the scale of 2–20 nm. This is an excellent scale range where the Porod's law is satisfactorily valid and includes the nanostructure under investigation. A deviation from linear line is observable at larger scale (the left-side of the curve illustrated in figure 3). This contributes the smallest nanofibers leading to higher SAXS intensity due to smooth surface of the individual nanofibers. At a larger scale, the SAXS data are not useful due to local differences and significant height differences in the sample.

However, fractal analysis at this specified scale range is completely satisfactory, since it represents nanostructure of smallest individual nanofibers bunched. It is of particular interest, since diffusion will occur within such tiny nanofibers. From the slope of

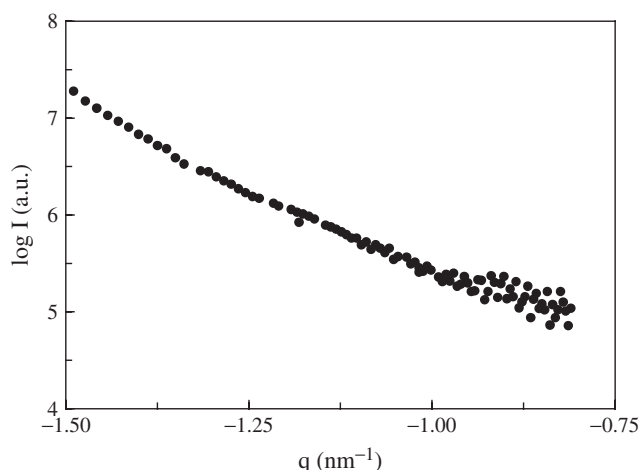


Figure 3. SAXS intensity $I(q)$ against the q factor plotted in logarithmic scale. The curve slope is equal to 3.1945.

the curve displayed in figure 3, one can estimate a fractal dimension of 2.81 for the upper surface of the flower-like bunches of $\text{LiV}_{0.1}\text{Mn}_{1.9}\text{O}_4$ nanofibers. This fractal dimension is very close to the theoretical dimension of a complete space i.e. 3. It is indeed indicative of a complicated 3D structure for the flower-like bunches of $\text{LiV}_{0.1}\text{Mn}_{1.9}\text{O}_4$ nanofibers. This corresponds to the fractal structure in the scale of few nanometers, which is of interest for diffusion process, as this is the porosity scale needed for diffusion of electroactive ions (diffusion in smaller channels is difficult and larger channels are useless wasting the space).

Although our emphasis was on the structural shape of this novel form of nanostructured materials, it can be easily concluded that this 3D structure is associated with a better diffusion process assisting to achieve the theoretical capacity of the electroactive materials [4]. It has been discussed that diffusion through tiny pores within the cathode materials is an efficient processes to improve the battery performance [25]. On the other hand, strong interaction of nanomaterials with lithium ions occurring at the surface rather than bulk causes an improvement in the high rate discharge capacity [26]. According to the recent advancement of statistical (non-equilibrium) thermodynamic aspect of electroactive materials involving diffusion processes [27, 28], it is possible to inspect this issue. This preliminary report with general form flattens the path for such future researches. In other words, it proposes a new case for surface studies.

4. Conclusion

Surface analysis of flower-like bunches of $\text{LiV}_{0.1}\text{Mn}_{1.9}\text{O}_4$ nanofibers revealed that they have complicated surface structure. According to fractal analysis performed by means of SAXS, a complicated 3D structure can be detected for them. In general, the results reported here introduce a new structure of nanostructured materials, which deserves

further attention from surface science point of view. Since the total size of such bunches are sufficiently large, study of their surfaces is an important task which should be performed via appropriate techniques of surface studies. Future research devoted to surface analysis of this novel nanostructured form (as started by this preliminary paper) will reveal very interesting features, which can be correlated with simultaneous results obtained from studies associated with materials properties (e.g. battery performance for this typical case).

References

- [1] C.R. Martin. Nanomaterials - A membrane-based synthetic approach. *Science*, **266**, 1961 (1994).
- [2] M.H. Huang, A. Choudrey, P.D. Yang. Ag nanowire formation within mesoporous silica. *Chem. Commun.*, **12**, 1063 (2000).
- [3] Y.-K. Zhou, J. Huang, H.-L. Li. Synthesis of highly ordered LiMnO_2 nanowire arrays (by AAO template) and their structural properties. *Appl. Phys. A*, **76**, 53 (2003).
- [4] A. Eftekhari. 3D Deposition of LiMn_2O_4 : enhancement of lithium battery performance. *Solid State Ionics*, **161**, 41 (2003).
- [5] N. Li, C.J. Patrissi, G. Che, C.R. Martin. Rate capabilities of nanostructured LiMn_2O_4 electrodes in aqueous electrolyte. *J. Electrochem. Soc.*, **147**, 2044 (2000).
- [6] C.R. Sides, N. Li, C.J. Patrissi, B. Scrosati, C.R. Martin. Nanoscale materials for Li-ion batteries. *MRS Bull.*, **27**, 604 (2002).
- [7] C. Sigala, D. Guyomard, A. Verbaere, Y. Piffard, M. Tournoux. Positive electrode materials with high operating voltage for lithium batteries: $\text{LiCr}_y\text{Mn}_{2-y}\text{O}_4$ ($0 \leq y \leq 1$). *Solid State Ionics*, **81**, 167 (1995).
- [8] H. Kawai, N. Nagata, M. Tabuchi, H. Tsukamoto, A.R. West. Novel 5 V spinel cathode $\text{Li}_2\text{FeMn}_3\text{O}_8$ for lithium ion batteries. *Chem. Mater.*, **10**, 3266 (1998).
- [9] A. Eftekhari. Electrochemical performance and cyclability of $\text{LiFe}_{0.5}\text{Mn}_{1.5}\text{O}_4$ as a 5 V cathode material for lithium batteries. *J. Power Sources*, **124**, 182 (2003).
- [10] Y.-K. Sun, C.S. Yoon, I.-H. Oh. Surface structural change of ZnO-coated $\text{LiNi}_{0.5}\text{Mn}_{1.5}\text{O}_4$ spinel as 5 V cathode materials at elevated temperatures. *Electrochim. Acta*, **48**, 503 (2003).
- [11] A. Eftekhari. Fabrication of 5 V lithium rechargeable micro-battery. *J. Power Sources*, **132**, 240 (2004).
- [12] R. Chitrakar, H. Kanoh, Y. Makita, Y. Miyai, K. Ooi. Synthesis of spinel-type lithium antimony manganese oxides and their Li^+ extraction/ion insertion reactions. *J. Mater. Chem.*, **10**, 2325 (2000).
- [13] A. Eftekhari. Improving cyclability of 5 V cathodes by electrochemical surface modification. *Chem. Lett.*, **33**, 616 (2004).
- [14] A. Eftekhari. Electrochemical behavior of thin-film LiMn_2O_4 electrode in aqueous media. *Electrochim. Acta*, **47**, 495 (2001).
- [15] A. Eftekhari, F. Moztarzadeh, M. Kazemzad. Flower-like microparticles of LiMn_2O_4 nanofibers, 207th ECS Meeting, May 15–20, Quebec, Canada, Abs#1352.
- [16] A. Eftekhari, F. Moztarzadeh, M. Kazemzad. Template-free preparation of bunches of aligned manganese oxide nanowires. *J. Phys. D: Appl. Phys.*, **38**, 628 (2005).
- [17] A. Eftekhari, M. Kazemzad, F. Moztarzadeh. A simple synthesis of manganese oxide nanowires. *Mendeleev Commun.*, **15**, 75 (2005).
- [18] A. Eftekhari, P. Jafarkhani, F. Moztarzadeh. Rectangular structure of manganese oxide nanowires. *Mater. Sci. Eng. B.*, **122**, 110 (2005).
- [19] M. Campos, B. Bello Jr. Small-angle X-ray-scattering investigation of poly(p-phenylene) with fractal properties. *Synth. Met.*, **60**, 1 (1993).
- [20] D.L. Williamson. Nanostructure of a-Si:H and related materials by small-angle. *Mater. Res. Soc. Symp. Proc.*, **377**, 251 (1995).
- [21] K. Tanaka, A. Ito, T. Yoshii, S. Suehiro, S. Nagura, N. Ando, Y. Hato. Fractal dimension analysis of polyacenic semiconductive (PAS) materials. *Carbon*, **39**, 1599 (2001).
- [22] W. Ruland. Apparent fractal dimensions obtained from small-angle scattering of carbon materials. *Carbon*, **39**, 323 (2001).
- [23] A. Eftekhari, M. Kazemzad, M. Keyanpour-Rad. Influence of atomic-scale irregularities in fractal analysis of electrode surfaces. *Appl. Surf. Sci.*, **239**, 311 (2005).
- [24] A. Eftekhari, M. Kazemzad, M. Keyanpour-Rad, M.A. Bahrevar. Quantitative surface analysis of plastic deformation of Pd electrodes in nanoscale. *Appl. Surf. Sci.*, **242**, 82 (2005).
- [25] A. Eftekhari. Aluminum oxide as a multi-function agent for improving battery performance of LiMn_2O_4 cathode. *Solid State Ionics*, **167**, 237 (2004).

- [26] S.H. Ye, J.Y. Lv, X.P. Gao, F. Wu, D.Y. Song. Synthesis and electrochemical properties of LiMn_2O_4 spinel phase with nanostructure. *Electrochim. Acta*, **49**, 1623 (2004).
- [27] A. Eftekhari. On the Onsager's phenomenological coefficient of Prussian blue electrochemical redox system. *Chem. Phys. Lett.*, **374**, 164 (2003).
- [28] A. Eftekhari. Variations of phenomenological coefficient of an electrochemical redox system in the course of cycling and aging. *Chem. Phys. Lett.*, **378**, 89 (2003).